

# Carbon Distribution in the Stillwater Complex and Evolution of Vapor During Crystallization of Stillwater and Bushveld Magmas

by E. A. MATHEZ<sup>1</sup>, V. J. DIETRICH<sup>2</sup>, J. R. HOLLOWAY<sup>3</sup>, AND  
A. E. BOUDREAU<sup>4</sup>

<sup>1</sup>*Department of Mineral Sciences, American Museum of Natural History, New York, NY 10024*

<sup>2</sup>*Institut für Mineralogie, ETH Zentrum, Zürich, CH-8092*

<sup>3</sup>*Departments of Chemistry and Geology, Arizona State University, Tempe, AZ 85287*

<sup>4</sup>*Department of Geological Sciences, University of Washington, Seattle, WA 98195*

(Received 17 January 1988; revised typescript accepted 21 July 1988)

## ABSTRACT

The occurrence and distribution of carbon in the Stillwater Complex have been investigated. In mineralized troctolite and associated rocks of olivine-bearing zone I (OBI), carbon is present as graphitic material and calcite. The assemblage forsterite-antigorite-calcite-graphite and the petrographic relations indicate equilibration of the carbon-rich phases during serpentinization. Typical OB I troctolite contains 500–1100 ppm wt. carbon, 40–70% of which is in calcite, whereas troctolite from higher stratigraphic positions generally contains <400 ppm carbon. Due to the metamorphism, it is not possible to deduce the extent to which enrichment of carbon in the ore zone is inherited from magmatic processes. In contrast, there is good evidence for magmatic graphite in parts of the Bushveld Complex.

The C–O–H–Cl system has been investigated for conditions of Stillwater and Bushveld crystallization. In alkali-poor fluids over a wide range of igneous and metamorphic conditions, the important chlorine species are HCl and CH<sub>3</sub>Cl. The addition of chlorine to a C–O–H fluid in equilibrium with graphite leads to a quantitative increase in HCl + CH<sub>3</sub>Cl and corresponding decrease in H<sub>2</sub>O contents, and, when Cl/H exceeds 1, to a CO<sub>2</sub> + CO-rich fluid with little H<sub>2</sub>O. Similarly, in more reduced fluids, CH<sub>4</sub> contents are depressed by the formation of CH<sub>3</sub>Cl.

From consideration of volatile solubilities and abundances in mafic magmas and the nature of the C–O–H–Cl system, it is hypothesized that the first fluid to exsolve from Bushveld and Stillwater intercumulus melt was composed of a mixture of CO<sub>2</sub>, CO, and HCl with minor amounts of sulfur species and H<sub>2</sub>O. A model is developed for the evolution of such a fluid with cooling. The model assumes that graphite began to precipitate from the fluid at supersolidus temperature and that the system cooled down a  $T-f_{O_2}$  path parallel to and > 2 log units below that of the Ni–NiO oxygen buffer. Upon the appearance of graphite, the fluid evolved to a more hydrogen-rich composition by graphite precipitation and loss of oxygen to the surrounding silicate-oxide assemblage. Cooling of fluid to 25 °C below the first appearance of graphite resulted in reduction in the fluid mass by > 70%, thus concentrating chlorine, sulfur and other residual species in the intercumulus fluid and melt. The model explains the presence of chlor-apatite and the enrichment of graphite in the Bushveld Critical Zone and predicts that chlor-apatite-bearing Stillwater rocks were similarly enriched in graphite during crystallization.

## INTRODUCTION

Histories of complex interactions between crystalline phases and volatile-rich melt and vapor are preserved in the Stillwater and Bushveld Complexes. Evidence for these

interactions include the presence of laterally-continuous, pegmatitic stratiform horizons (e.g., the Merensky and Howland Reefs) and more local discordant bodies (Raedeke & McCallum, 1984; Viljoen & Scoon, 1985); postcumulus chlorine-rich apatite, biotite, and hornblende (Boudreau *et al.*, 1986); and abundant graphite in some of the pegmatitic and sulfide-rich rocks (Volborth & Housley, 1984; Ballhaus & Stumpfl, 1985). The high-temperature vapor is of interest because it may be an important agent for geochemical transport. For example, it has been speculated that magmatic vapor was in part responsible for the concentration of platinum group elements (PGEs) in the Merensky and Howland Reefs (e.g., Lauder, 1970; Vermaak, 1976; Boudreau *et al.*, 1986).

Vapor must initially form by exsolution from intercumulus melt. The composition of this first vapor and how it evolved during crystallization are not well constrained because its composition is determined by the relative solubilities of the volatile elements in the melt. In addition, it is not clear how the vapor evolved as it interacted with the crystal-melt assemblage during cooling to subsolidus temperature. One problem is that most of the minerals from which near-solidus conditions could be inferred have re-equilibrated during cooling. This problem is aggravated by the fact that in the subsolidus environment fluids may be introduced from external sources. The difficulties are illustrated in part by the large range in fluid-inclusion compositions represented in the Bushveld Complex (Ballhaus & Stumpfl, 1986).

One possible means of deducing volatile behavior at solidus and supersolidus conditions in layered intrusions is by the study of the condensed carbon-rich phases. Accordingly, in this paper the occurrences and distribution of carbon in the Stillwater Complex are reported and compared with those in the Bushveld Complex. The significance of these occurrences with respect to high-temperature conditions is evaluated. The observations on carbon are combined with those on halogen-bearing minerals, with computations illustrating the nature of C–O–H–Cl fluids, and with melt-vapor relationships known from experiment and observations of natural systems to develop a general model for fluid evolution from Stillwater and Bushveld magmas. The terms vapor and fluid are used synonymously to denote the low-density phase composed primarily of volatile molecules at supercritical temperature.

## CARBON IN THE STILLWATER COMPLEX

### *Petrography and occurrence*

In mineralized troctolites and associated rocks of olivine-bearing Zone I (OB I) (Fig. 1), the carbon-rich minerals, where they can be observed, consist of variable proportions of calcite and graphitic material. The latter have been observed as a film on crack, grain boundary and cleavage surfaces in OB I and other Stillwater rocks studied in detail (Fig. 2). Graphitic material is particularly apparent with sulfides and as flakes in cleavage planes of phlogopite and serpentine. It is not known whether the carbonaceous material in cracks is dominantly graphitic or whether it also consists of low-temperature organic compounds, such as those present in cracks in peridotite xenoliths from alkalic basalts (Mathez, 1987). In any event, the distribution clearly indicates that on a microscopic scale the carbonaceous material was deposited late in the paragenetic sequence. In the Picket Pin Zone near the top of AN II (Boudreau & McCallum, 1986), carbonaceous material is associated with alteration of the igneous assemblage. Calcite is present as a rare space-filler to cumulus plagioclase and is also associated with alteration and post-solidification veins.

Macroscopic masses of graphite have not been observed in OB I rocks. However, massive graphite has been reported by Volborth & Housley (1984) in pegmatoidal pyroxenite near

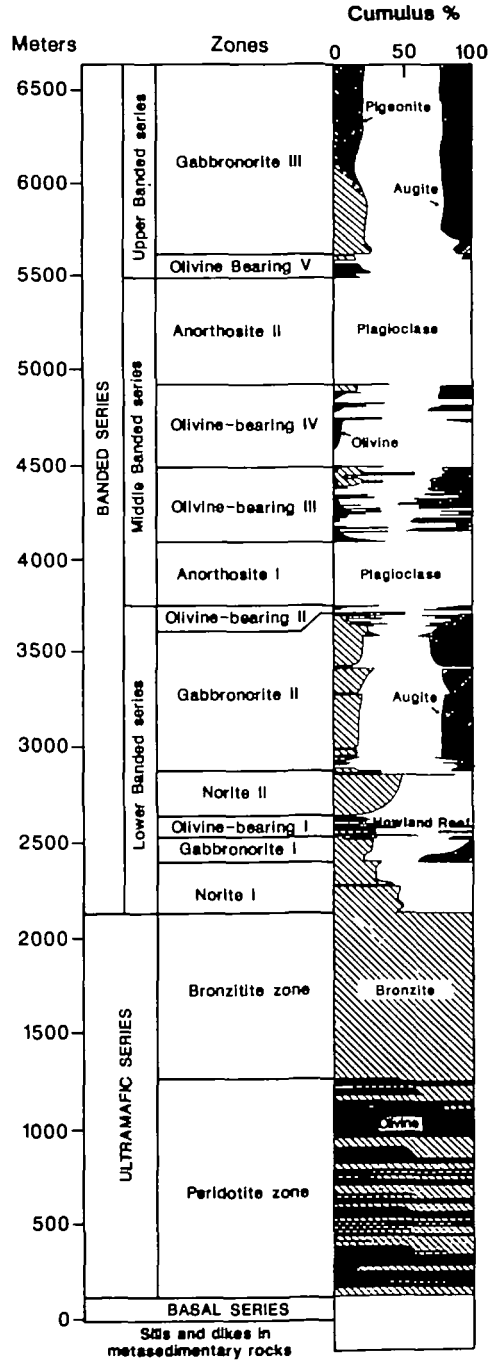


FIG. 1. Composite stratigraphic section of the Stillwater Complex of McCallum *et al.* (1980) and Raedeke & McCallum (1984) showing the stratigraphic position of the olivine-bearing horizons of the Banded Series.

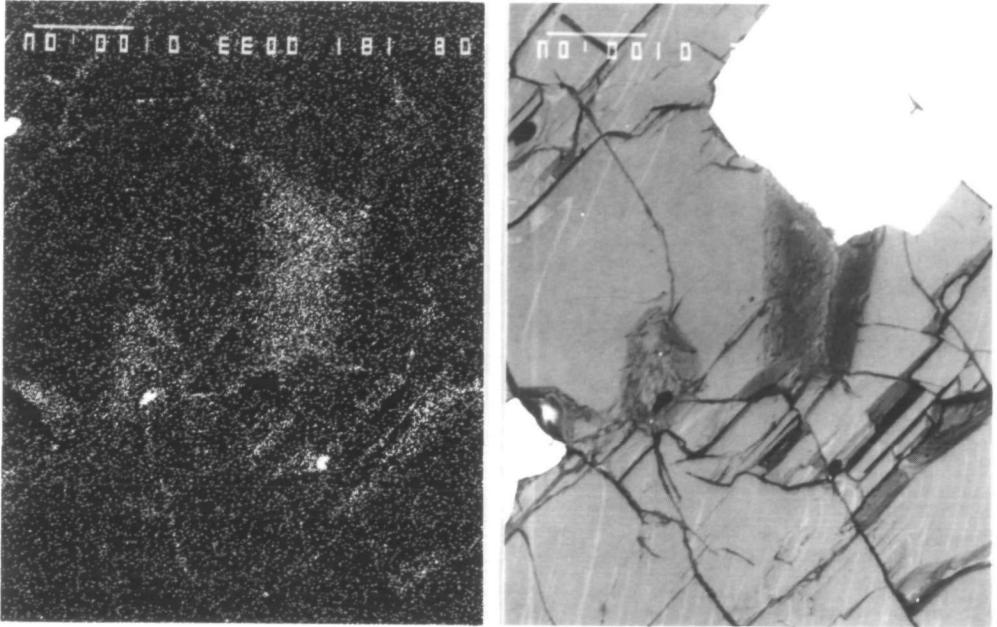


FIG. 2. Backscatter electron (top) and carbon X-ray (bottom) micrographs of a polished surface of a sample of the G chromitite, Stillwater Complex. The white (high Z) phase is chromite, which is surrounded by olivine. A portion of the chromite was plucked out during polishing, exposing the chromite–olivine grain boundary. It can be seen that a carbon film is present on this and the exposed cleavage and crack surfaces. Discrete carbonaceous grains are also visible in the X-ray micrograph and appear as discrete, dark spots in the backscatter electron micrograph. The vertical bar on each micrograph represents 100  $\mu\text{m}$ . The sample is coated with aluminum.

the base of the Banded Series 300–500 m stratigraphically below OB I. They report that the pyroxenites form a 'stockwork' in noritic and gabbroic rocks, that the graphite is associated with sulfides in 'smaller cross-cutting vein, pipe, and breccia-like structures' surrounded by magnetite-bearing rocks in the pyroxenites and that graphite is associated with sulfides, arsenides, carbonate, and serpentine.

Obviously, if graphite precipitated at near-solidus temperatures, the petrographic evidence has been obliterated by metamorphism. In fact, the assemblage forsterite–antigorite–calcite–graphite, which characterizes the troctolites of OB I, is stable only below 510°C at 3 kb and moderate  $f_{\text{O}_2}$  in CaO–MgO–SiO<sub>2</sub>–H<sub>2</sub>O–CO<sub>2</sub> bulk compositions (Trommsdorff & Evans, 1977). Therefore, the mere presence of calcite in these partially serpentinized rocks demands redistribution of carbon at least on the scale of the grain size of the troctolite. The influence of metamorphism on carbon distribution is considered below.

#### *Sampling and analytical procedures for carbon analysis*

In order to document the megascopic distribution of carbon, selected Stillwater rocks were analyzed. Sampling and subsequent analysis were conducted so that the extent of metamorphic redistribution on several scales could be documented. The sampling was also designed to avoid anomalously carbon-rich rocks, such as the graphite-rich ones described by Volborth & Housley (1984) and highly-altered, calcite-rich ones occasionally encountered in the Banded Series. Relatively fresh samples were chosen for bulk analysis, most of which were collected either from the Minneapolis adit or from fresh outcrop in the Picket

Pin and Contact Mountain areas. It should be emphasized, however, that nearly all Stillwater troctolites, especially those from the Minneapolis adit, are at least partially serpentinized.

Approximately half of the samples analyzed were collected specifically for this study and have masses of 2–3 kg. Homogeneity on this scale was evaluated by analysis of two or three fragments (typically 10–30 g each) of each sample. The variability exhibited by these multiple analyses was generally found to be less than the variability among analyses of different samples collected from different outcrops. Therefore, there is no evidence for the development of compositional heterogeneity during metamorphism on the scale represented by kilogram-size samples. Other samples used in this study were smaller (< 500 mg), originally having been collected for other purposes, and only one analysis of each was made.

The preparation and analytical procedures are described in detail elsewhere (Mathez, *et al.*, 1984). Briefly, samples were crushed in steel and agate to pass through a 1.4 mm sieve, with the < 1.4 mm size fraction being removed periodically to minimize the proportion of small grain sizes. The crushed samples were split into two fractions, one of which was washed in water and the other in cold 1N HCl for several minutes to permit determination of the proportion of calcite carbon to total carbon. As noted in previous work, it is estimated that only 80–90% of the calcite is removed by this procedure, the problem with harsher leaching procedures being that part of the noncarbonate fraction may also be removed. The point of the acid wash is to show gross distinctions in the proportions of calcite to total carbon and to identify those samples in which high carbon contents are due primarily to high calcite contents. Carbon was analysed with a Coulomat C analyzer at the ETH, Zürich. Samples were fused with a Li-tetraborate flux in oxygen at 1250 °C, and the amount of CO<sub>2</sub> liberated was determined by a coulometric-alkalimetric titration technique (Sixta, 1977).

### *Abundances*

The abundances of carbon in Stillwater rocks are summarized in the histograms of Fig. 3a. The histograms are of 107 individual samples rather than of the 185 analyses of different splits from these samples, but the distribution defined by the latter is similar. It can be seen that the carbon contents of all but one of the troctolites from OBI range from 500 to 1100 ppm wt., whereas most troctolites from higher stratigraphic positions contain less than 400 ppm carbon. The two most carbon-rich samples among the latter group contain high proportions of calcite, are more altered than other samples and are therefore judged not to be significant with respect to the overall distribution. It is also evident in Fig. 3a that the OBI troctolites are enriched in carbon compared to associated norites and anorthosites. However, both the anorthositic as well as olivine-bearing lithologies of OBI are more carbon-rich than similar rocks from higher in the intrusion.

For the Picket Pin anorthosites near the top of AN II (Boudreau & McCallum, 1986), no significant differences in carbon abundances are observed between sulfide-bearing and sulfide-free samples. The carbon contents of most of these rocks are extremely low. They also possess much lower proportions of calcite carbon to total carbon than the troctolites or leucocratic rocks from other stratigraphic positions (Fig. 3b).

The data indicate that carbon abundance is higher in the stratigraphically lower part of the Stillwater Complex than in its upper portion. Furthermore, abundances in OB I rocks are generally higher than anticipated based on the low carbon solubilities in silicate melts (see below) and the fact that the rocks are cumulates. Therefore, carbon must have been enriched by magmatic (e.g., precipitation of graphite from magmatic vapor) or metamorphic

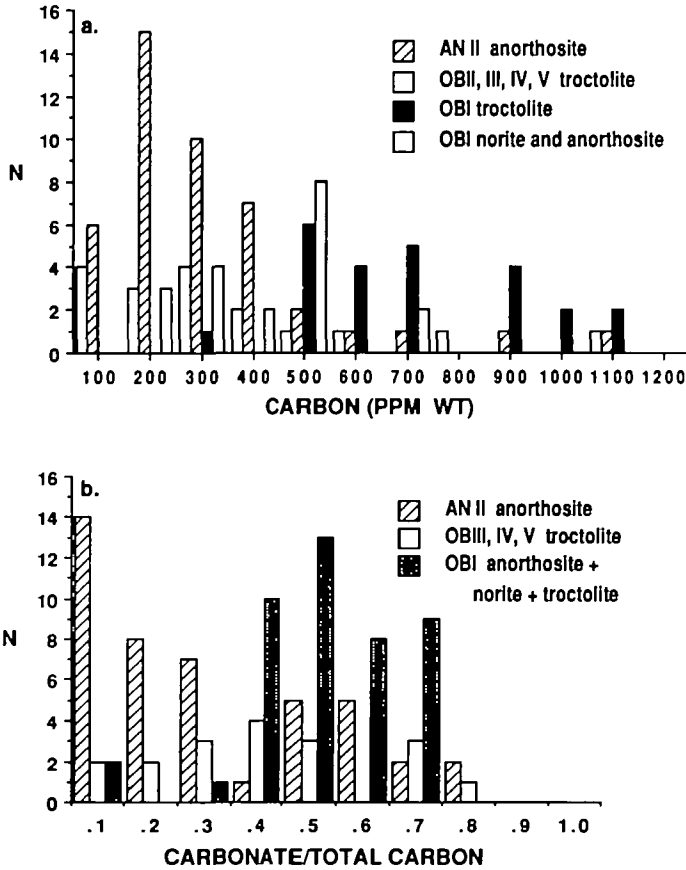


FIG. 3. Histograms of: (a) total carbon contents; and (b) carbonate/total carbon ratios of Stillwater rocks. Most analyses represent averages of analyses of two or three fragments of kilogram-size samples (see text). The stratigraphic nomenclature is that of McCallum *et al.* (1980).

processes. Before considering the former, it is appropriate to evaluate the extent to which the observed variation may be an artifact of metamorphism.

*Effects of metamorphism on carbon distribution*

*Nature of metamorphism*

The Stillwater Complex has been subjected to an incipient and localized greenschist facies metamorphism. Whether or not the metamorphism occurred during or subsequent to initial cooling, it must have involved influx of water-rich fluid from a source external to the most intensely metamorphosed rocks. This is indicated by the presence of tremolitic veins and the fact that Stillwater troctolites are partially serpentinized, which requires relatively large quantities of water (see below). The secondary assemblages in the anorthosites, norites and gabbros include, depending on the specific mafic minerals present, prehnite (+ pumpellyite), albite + clinozoisite ± chlorite ± clinoamphibole, and tremolite + talc + chlorite (McCallum *et al.*, 1980). The different Banded Series troctolites themselves are characterized by different metamorphic assemblages. OBI olivine is partially altered to antigorite + magnetite, and

olivine of the stratigraphically higher OB V is locally altered to talc + tremolite surrounded by chlorite rims. The intensity of metamorphism is extremely variable. Individual thin sections commonly include fresh regions with interspersed millimeter- to centimeter-size patches of completely altered minerals. On the outcrop scale alteration is clearly most intense around megascopic fractures, which thus must have served as the main channels for infiltrating metamorphic fluids (McCallum *et al.*, 1980).

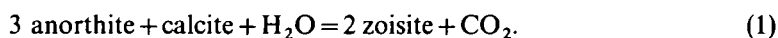
#### *Infiltration and circulation of fluid during cooling*

Despite the greenschist facies metamorphism, two observations suggest that during initial cooling to temperatures at least down to 600 °C there was no significant permeability to fluid along grain boundaries or microcracks. First, Dunn (1986) found that the igneous minerals and fresh whole rocks retained their magmatic  $\delta^{18}\text{O}$  signatures. Second, Boudreau *et al.* (1986) showed that Stillwater and Bushveld phlogopites possess highly variable chlorine/fluorine ratios which, contrary to expectation, are not closely correlated to the crystal-chemical parameters known to exert a strong influence on that ratio. (The amount of chlorine that can be incorporated into phlogopite increases with increasing contents of small tetrahedral or large octahedral cations, i.e. higher Si/Al or  $\text{Fe}^{2+}/\text{Mg}$ .) This was interpreted to mean that phlogopite equilibrated at subsolidus temperature with pore fluids of variable composition, which in turn implies that, in order to maintain fluid heterogeneity, permeabilities must have remained low during much of the subsolidus cooling history except near megascopic channelways such as veins.

These observations suggest that there was no movement of carbon in or out of Stillwater rocks as they cooled at high temperature. However, it is necessary to consider the greenschist effects on carbon-bearing phases. Based on the observed assemblages, there are two relevant reactions.

#### *Breakdown of calcite*

Anorthite and calcite break down to zoisite in the presence of water-rich fluid according to the reaction (Allen & Fawcett, 1982),



Thus, even weakly metamorphosed anorthositic rocks may have lost part of their original carbon. Clinozoisite is present in many leucocratic Stillwater rocks, including the Picket Pin anorthosites (Boudreau & McCallum, 1986). As noted above, the carbon contents of these rocks are extremely low, and they contain much lower proportions of calcite carbon to total carbon than other analyzed samples (Fig. 3b). These features are consistent with loss of carbon according to reaction (1).

Clinozoisite is also locally present in the leucocratic rocks of OB I. However, in these and associated troctolites, calcite usually constitutes 40–60% of the total carbon (Fig. 3b). Therefore, in contrast to the Picket Pin rocks, those of OB I exhibit no evidence for breakdown of calcite and large-scale loss of  $\text{CO}_2$ .

#### *Serpentinization*

The serpentinization process is potentially important because it involves transfer of large amounts of fluid and strongly influences oxidation equilibria, which may in turn affect the relative stabilities and amounts of calcite and graphite. The specific variations in  $f_{\text{O}_2}$  accompanying serpentinization of peridotites has been examined in detail by Frost (1985), and the generalized topology for such a system is reproduced in Fig. 4. The relevant mass

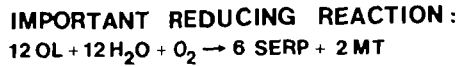
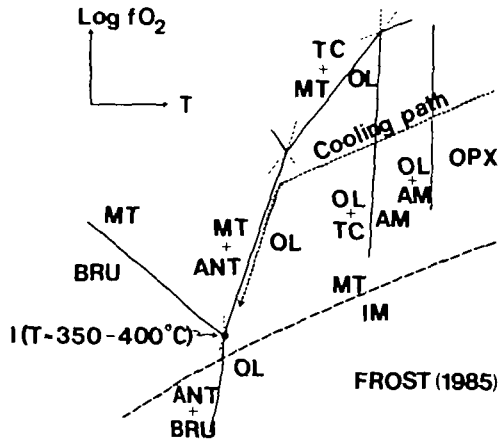
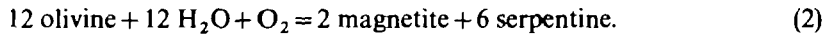


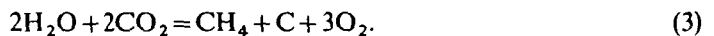
FIG. 4. Reaction relationships in the system Si-Mg-Fe-O-H, adapted from Frost (1985), illustrating the influence of serpentinization reactions on  $f_{\text{O}_2}$ . The presumed cooling path of a typical mafic system is shown. The invariant point I is estimated by Frost to be 5–6 orders of magnitude below NNO and thus falls within the stability field of graphite. The extent of reduction due to breakdown of olivine will depend on the fluid-rock mass ratio. AM = amphibole; ANT = antigorite; BRU = brucite; IM = iron metal; MT = magnetite; OL = olivine; OPX = Ca-poor pyroxene; TC = talc.

balance, as written by Frost, is

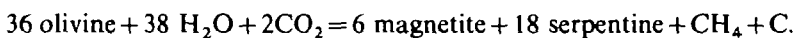


The stoichiometry here is determined in part by the specific mineral compositions, which Frost chose to be representative of ultramafic systems. If allowed to go to completion and not overwhelmed by infiltration of large quantities of oxidized fluid, reaction (2) would continue to the invariant point I (Fig. 4), after which continued introduction of fluid and breakdown of the iron oxides to hydroxides would drive the system back to more oxidizing conditions. Frost (1985) estimates that for typical peridotite bulk compositions, I lies 4 to 5 orders of magnitude below the  $f_{\text{O}_2}$  of the nickel–nickel oxide buffer (NNO) at a temperature of 350–400°C, or well within the field of graphite stability.

As noted above, most OBI troctolites contain the assemblage forsterite–antigorite–calcite–graphitic material. Therefore, it is necessary to consider whether or not the serpentinizing fluid itself could have been a source of carbon. Reaction (2) is written to emphasize the consumption of oxygen. As it proceeds to the right, the oxygen necessary for crystallization of magnetite is supplied by the fluid. The expression for the breakdown of fluid to produce graphite can be represented as



Combining reactions (2) and (3) to eliminate oxygen yields



Obviously troctolites may become enriched in carbonaceous material and fluids in  $\text{CH}_4$  in this way. On a mole for mole basis the maximum amount of graphite that could precipitate is 1/36 of the amount of olivine consumed. This quantity is maximum because if large quantities of oxidized fluid flowed through the rocks, graphite-saturation may never have



been reached. In this case, the  $f_{O_2}$  of the system would have been controlled by the fluid itself, which would have represented an infinite oxygen reservoir. This possibility was explicitly recognized by Frost (1985), who emphasized that reduced conditions can only be achieved during serpentinization if either the mass of metasomatizing fluid is much less than the mass of rock or the fluid itself is initially reducing ( $CH_4$ -rich). Thus, even though serpentinization reactions involve large quantities of fluid and tend to reduce the rocks, they need not lead to solution or crystallization of either calcite or graphite, and the amounts of graphite in troctolitic rocks will depend on the balance between the extent of serpentinization and the amount of oxidizing fluid flowing through the rock.

The average carbon contents of OB I troctolites and leucocratic rocks are approximately 700 and 500 ppm, respectively. The above analysis demonstrates that it is not possible to deduce from the existing abundance data, textures, or assemblages to what extent these concentrations are artifacts of original magmatic processes. For this reason, it is useful to consider the Bushveld graphite occurrences.

### BUSHVELD GRAPHITE

Graphite appears to be much more common in the upper Critical Zone of the Bushveld Complex than in the lower Banded Series of the Stillwater Complex. Its ubiquitousness and close association with Bushveld ore, both in stratiform horizons and in the pipes, was first emphasized by Wagner (1924, p. 105), who could not "remember handling a single specimen of ore in which careful search failed to reveal the presence of some graphite (and that) there is thus unquestionably some relation between the distribution of graphite and that of ore . . ." He also noted that graphite was not observed in 'barren' Bushveld rocks.

Wagner, and later Schneiderhöhn (1929), recognized that some of the Bushveld graphite formed at supersolidus temperature. For example, Schneiderhöhn (1929) pointed out that graphite is associated with intercumulus patches of hornblende, biotite and sulfide in Merensky rocks. He considered the assemblage to have resulted from reaction of 'readily fugitive compounds' concentrated in a residual interstitial magma. Similar observations have been reported by Ballhaus & Stumpfl (1985), who also argued for a magmatic origin for some graphite. Such petrographic relations have not been observed in Stillwater rocks, perhaps because they have been obliterated by metamorphism.

Ballhaus & Stumpfl (1985) and Ballhaus (1988) reported pegmatitic rocks consisting of more than 80% graphite in the Bastard Reef, which is approximately 9 m stratigraphically above the Merensky Reef, and similar occurrences are well-known to the mine geologists at Rustenburg. The low subsolidus permeability of these rocks (noted above) and the fact that massive graphite appears to be specifically associated with stratiform igneous pegmatoids (Ballhaus & Stumpfl, 1985) also imply that the graphite is igneous. These stratiform occurrences should be distinguished from the massive graphite associated with the discordant Bushveld pipes (Stumpfl & Rucklidge, 1982), which are believed to be replacement bodies (Schiffries, 1982), and the occurrences described by Volborth & Housley (1984) in Stillwater rocks. How the graphite in these discordant bodies formed is not obvious, and since they have not been studied they will not be considered further.

### SIGNIFICANCE OF STILLWATER AND BUSHVELD CARBON

It has been shown that the Stillwater OB I troctolites contain more carbon than similar lithologies higher in the complex but that metamorphism has obliterated any indication of what may have been the original nature and distribution of carbon in the Complex.

Although there has been no systematic study of the distribution of carbon throughout the Bushveld Complex, the descriptions summarized above leave little doubt that portions of the Upper Critical Zone are also enriched in graphite and that some of the graphite is magmatic. The large-scale distribution of carbon in both complexes appears to be similar, suggesting the possibility that the Stillwater ore zone was also enriched in carbon by magmatic processes. The high-temperature precipitation of graphite must reflect interactions of a carbon-rich magmatic vapor and the condensed assemblage. The manner in which the magmatic vapor evolved in a partially molten cumulate pile is therefore explored in the following sections.

## FLUIDS OF C-O-H-Cl COMPOSITION

### *Method of computation*

For reasons stated below, the first vapor to exsolve from Stillwater and Bushveld magmas may be approximated by a mixture of C-O-H-Cl species. In order to understand how the presence of chlorine influences graphite stability, speciation in this system has been computed for the temperature and pressure ranges of 1200–600°C and 1000–5000 b, respectively.

Computations were made using a free-energy minimization procedure (Gordon & McBride, 1971; Holloway & Reese, 1974), and equilibria were considered among all the species listed in the JANAF tables. Fugacity coefficients for end-member species were computed from the modified Redlich-Kwong equation-of-state (Holloway, 1981). As for other equations-of-state based on the theory of corresponding states, the Redlich-Kwong formulation is strictly suitable for fluids consisting of non-polar, spherical molecules, so computations of the properties of other fluids are only approximations. Mixing of the species was taken to be ideal. For the C-O-H system, the additional consideration of non-ideal mixing of species does not significantly influence computed fluid compositions for the conditions of interest here. The assumption of ideal mixing is further justified because there is no basis to assert that non-ideal mixing computed from the mixing rules yields a more accurate representation of complex C-O-H-Cl fluids (Prausnitz *et al.*, 1986).

### *C-O-H-Cl fluids on the graphite surface*

The shape of the graphite surface in the C-O-H-Cl system (Fig. 5a) reflects the fact that the major chlorine-bearing species in the system are Cl<sub>2</sub>, CCl<sub>4</sub> (tetrachloromethane), COCl<sub>2</sub> (carbonyl chloride), HCl and CH<sub>3</sub>Cl (chloromethane). It can be seen that the graphite surface extends from nearly pure HCl to intermediate species on the C-O, C-H, and C-Cl joins. The curvature of the surface near the C-H join is due to the stability of CH<sub>3</sub>Cl, and most fluids near the C-O-H face are mixtures of HCl, CH<sub>3</sub>Cl, and the C-O-H species. The latter include CO<sub>2</sub>, CO, and H<sub>2</sub>O on the oxidized side of the face and H<sub>2</sub> and CH<sub>4</sub> on the reduced side (Holloway, 1981). CCl<sub>4</sub> is important only through a limited compositional range in the vicinity of the C-Cl join, and Cl<sub>2</sub> and COCl<sub>2</sub> are major species only in hydrogen-poor fluids having compositions near the C-O-Cl face. For example, on that face at 1000°C and 3000 b, COCl<sub>2</sub> reaches a maximum concentration of 25.2% at Cl/(Cl + O) = 0.67.

The graphite surface illustrated in Fig. 5a is for 1200°C and 3000 b. Temperature and pressure have little effect on its position throughout the ranges examined. As temperature decreases, for example, the graphite surface migrates toward CO<sub>2</sub>, CH<sub>4</sub>, and CCl<sub>4</sub> on the joins emanating from the C apex and toward H<sub>2</sub>O on the C-O-H face, but it remains fixed

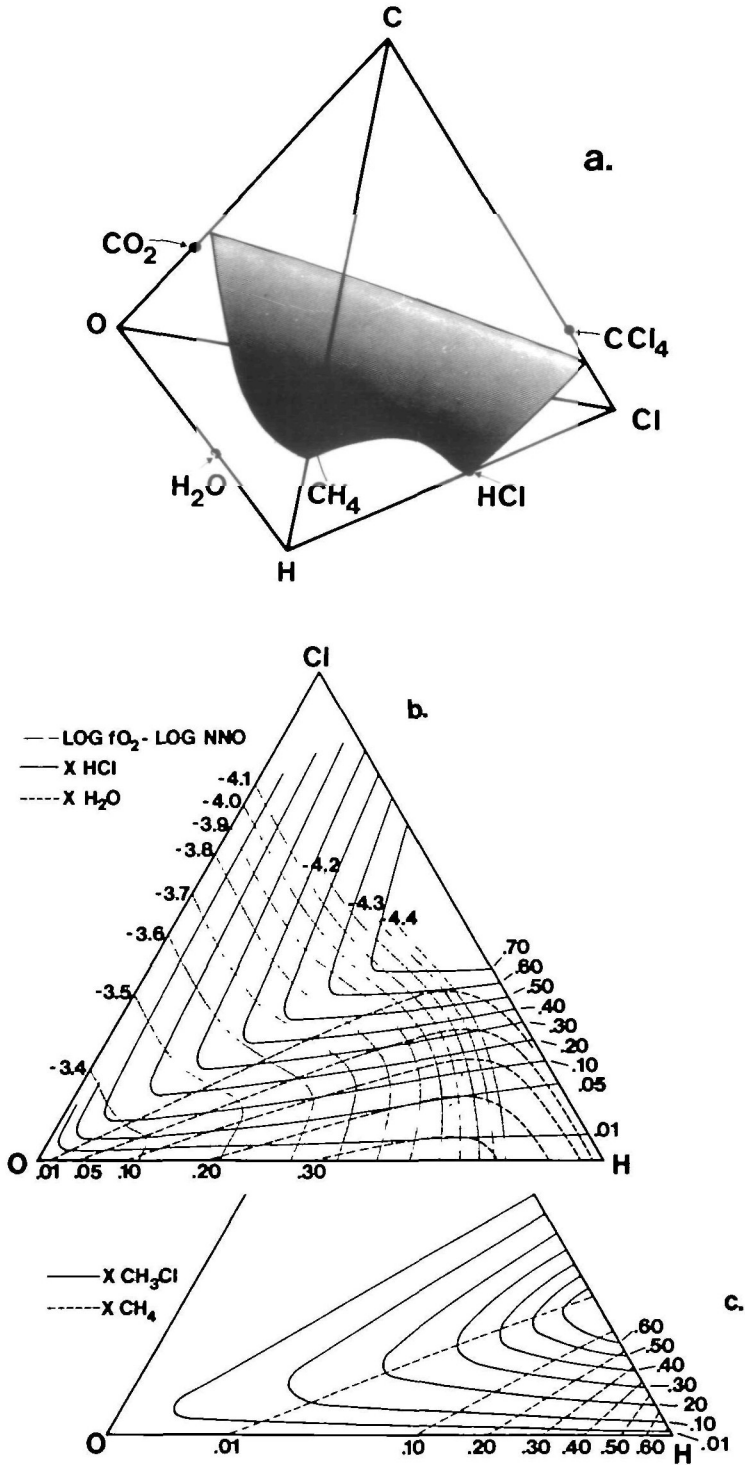


FIG. 5. The graphite saturation surface in the C-O-H-Cl system at 1200°C, 3 kb. (a) In perspective. (b) The surface projected from the C apex and contoured for  $X_{\text{HCl}}$ ,  $X_{\text{H}_2\text{O}}$  and  $\log f_{\text{O}_2}$  [expressed as the difference  $\log f_{\text{O}_2} - \log f_{\text{NiO}}$  of the Ni-NiO buffer ( $10^{-7.51}$  b)]. (c) The same surface contoured for  $X_{\text{CH}_3\text{Cl}}$  and  $X_{\text{CH}_4}$ .

near HCl on the C–H–Cl face. Again, this implies that throughout a wide range of igneous and metamorphic conditions C–O–H–Cl fluids can be regarded as mixtures of C–O–H species with HCl and/or CH<sub>3</sub>Cl. How C–O–H fluids vary with temperature and pressure has been examined in detail by Holloway (1981, 1984).

Illustrations of the graphite surface contoured for  $f_{O_2}$  and mole fractions of H<sub>2</sub>O, HCl, CH<sub>3</sub>Cl, and CH<sub>4</sub> are presented in Fig. 5b and c. Of interest is the fact that except in the immediate vicinity of H<sub>2</sub>O the most abundant hydrogen-bearing species is HCl and/or CH<sub>3</sub>Cl rather than H<sub>2</sub>O. The addition of chlorine to a C–O–H fluid leads to an essentially quantitative decrease in its H<sub>2</sub>O and increase in its HCl + CH<sub>3</sub>Cl contents. This is illustrated further by comparison of Fig. 6a and b. As hydrogen content increases from left to right on Fig. 6b, HCl displaces COCl<sub>2</sub> and Cl<sub>2</sub> as the most abundant chlorine species, the HCl content increases until all chlorine is combined as HCl, and only when the amount of atomic hydrogen exceeds atomic chlorine does H<sub>2</sub>O form. In more reduced systems, fluid CH<sub>4</sub> contents are also significantly depressed by the formation of CH<sub>3</sub>Cl (cf. Fig. 6a and b). The effect of decreased temperature is to increase H<sub>2</sub>O and CH<sub>4</sub> contents at the expense of CH<sub>3</sub>Cl (Fig. 6c). Increased pressure influences the system in the same way as decreased temperature, except that the effect is much less pronounced. In C–O–H fluids not in equilibrium with graphite, HCl and CH<sub>3</sub>Cl are the only major chlorine species, their ratios depending on  $f_{O_2}$ .

The curvature of the oxygen isopleths on the graphite surface (Fig. 5b) is also due to the stability of HCl relative to H<sub>2</sub>O. The practical effect is that the stability of graphite in natural systems is not strongly influenced by variations in fluid HCl contents for bulk compositions near the C–O–H face. However, just as CO<sub>2</sub>/H<sub>2</sub>O ratios of fluids in equilibrium with graphite are extremely sensitive to  $f_{O_2}$  (Fig. 6a), so too are their CO<sub>2</sub>/HCl and CO<sub>2</sub>/CH<sub>3</sub>Cl ratios (Fig. 6b).

Alkalis, alkaline earths, and some transition metals are known to form neutral chloride species in high-temperature aqueous fluids, so these elements should affect the equilibria described above. Webster & Holloway (1988) showed that chlorine partitioning between fluid and topaz rhyolite melt depends strongly on the chlorine, iron and alkali contents of the melt, among other variables. They suggested that fluid-melt equilibrium is described by a reaction such as



(M = metal, v = vapor and m = melt), and their solubility data indicate that HCl is present in the fluid only to the extent that its molar chlorine content exceeds the sum of molar alkali and iron contents. Given the complex dependency of chlorine solubility on compositional parameters of the melt (Webster & Holloway, 1988), it is not clear how the partitioning behavior of elements that potentially form chloride complexes between fluids and mafic melts can be inferred from data on granitic systems. It should be understood, however, that alkali and metal chlorides will act as inert dilutants in C–O–H fluids, that HCl and CH<sub>3</sub>Cl fluid contents will in general be lower when metal chlorides are present than when they are absent, and thus that these chlorides will in part mitigate the effects of chlorine on C–O–H equilibria.

#### EVOLUTION OF VAPOR FROM STILLWATER AND BUSHVELD MAGMAS

To the extent that the evolution of vapor from magma is controlled by fundamental physiochemical processes rather than by small differences in magma compositions, a model

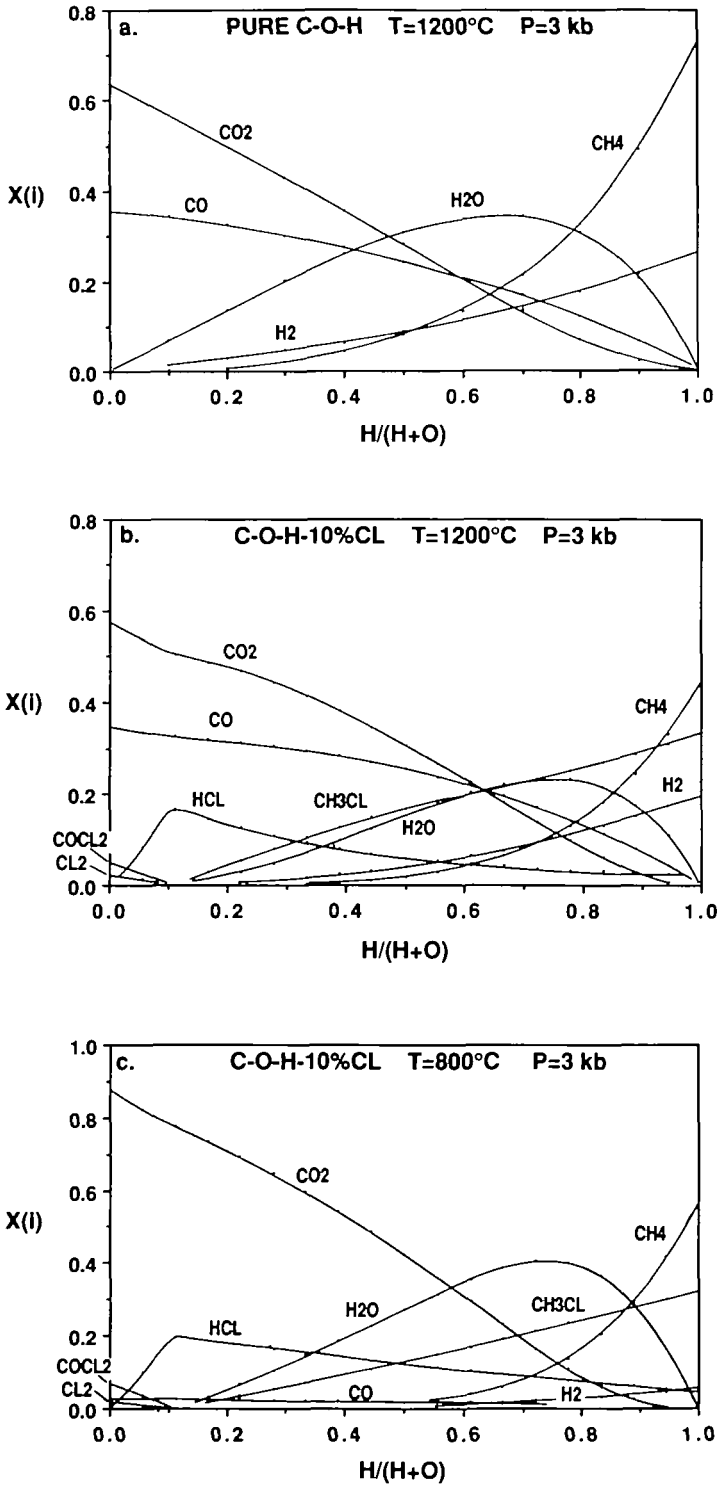


FIG. 6. Compositions of graphite-saturated fluids. (a) Pure C-O-H fluid and (b) and (c) fluids on the plane (C-(O+10%Cl)-(H+10%Cl).

for the evolution of magmatic vapor should be equally applicable to the Bushveld and Stillwater Complexes. Such a model must explain the presence of igneous graphite in the Bushveld and its inferred presence in the Stillwater as well as the chlorine-rich postcumulus apatites in the lower portions of both complexes (Boudreau *et al.*, 1986). Based on the known distribution behavior of the halogens among the relevant phases, the apatite compositions were interpreted to indicate that chlorine-rich fluids exsolved during crystallization of intercumulus melt in the Stillwater Lower Banded Series and Bushveld Upper Critical Zone (Boudreau *et al.*, 1986). The specific nature of the first vapor to separate from intercumulus melt and how it evolves with cooling depend primarily on the relative solubilities of the volatile elements in the magma, the initial  $f_{O_2}$  of the system and how  $f_{O_2}$  changes with cooling.

#### *Solubility constraints*

At pressures of 3–4 kb, the solubility of carbon in basaltic melts in equilibrium with  $CO_2$  is probably in the range 300–600 ppm wt. carbon (1200–2200 ppm  $CO_2$ ), judging from the data of Stolper & Holloway (1988). In contrast, the solubility of  $H_2O$  under similar conditions is 6–9 wt.%, depending on melt composition (Burnham, 1979). These contrasting solubilities account in part for the presence of nearly pure  $CO_2$  vesicles in submarine basalt glasses containing several tenths of a percent  $H_2O$  (Pineau *et al.*, 1976; Moore *et al.*, 1977). Peridotite xenoliths from alkali basalts offer a similar but more extreme example of contrasting glass and vapor compositions. Peridotites may contain inclusions of nearly pure  $CO_2$  trapped at pressures > 10 kb (e.g., Bergman & Dubessy, 1984), and some of these rocks also contain interstitial pockets of glass containing 2–5 wt.%  $H_2O$  (Irving & Mathez, 1982).

Although sulfur species are usually important constituents of volcanic gases (Gerlach & Nordlie, 1971), their solubilities in melts are much higher at pressures greater than several hundred bars than at 1 b. Thus, in lavas quenched at pressures of the deep ocean, most of the sulfur is dissolved in the glass, the amounts of sulfur dissolved in mafic magma and coexisting vapor being controlled by sulfide melt–silicate melt equilibria (Moore & Fabbri, 1971; Mathez, 1976). In an attempt to estimate the amounts of sulfur originally in the vesicles of these lavas, Moore *et al.* (1977) assumed that the vesicle gas had contained all of the sulfur now present in the sulfides lining the vesicle walls. Their analysis suggested that sulfur constitutes 4–6% of the magmatic vapor of MORBs. Under the conditions of interest here, sulfur will exist in the vapor as  $SO_2$ ,  $S_2$ , and  $H_2S$ , the relative proportions of which depend on  $f_{O_2}$  (Mathez, 1984), and consequently sulfur will affect C–O–H–Cl equilibria. However, because of their low concentrations in the vapor and the nature of the arguments that follow, it is assumed that the sulfur species behave as dilutants, and they will not be included in the following analysis.

For chlorine species, the only data on basaltic systems are those of Iwasaki & Katsura (1967), and these data are not sufficient to predict how chlorine distributes itself between melt and vapor. In addition, abundances of chlorine in lavas are highly variable and known to be correlated with potassium and phosphorous. For example, while the chlorine contents of MORBs and other tholeiitic glasses are usually < 200 ppm (Anderson, 1974; Unni & Schilling, 1978), other studies suggest that some mafic magmas contain thousands of ppm chlorine (Sigvaldason & Oskarsson, 1976, 1986; Devine *et al.*, 1984; Falloon & Green, 1986). Thus, although the Stillwater and Bushveld intercumulus melts were probably also chlorine-rich, there is no basis for estimating the chlorine contents of coexisting vapors. The model vapor considered below is arbitrarily assumed to contain 10 at.% HCl.

### *Oxygen fugacities*

The equilibria among fluid species and the temperature and rate of graphite precipitation are sensitive to the initial  $f_{\text{O}_2}$  and how it changes with cooling. Although mafic magmas should become more oxidized during perfect fractional crystallization (Carmichael & Ghiorso, 1986), it has generally been observed that  $T$ - $f_{\text{O}_2}$  paths followed by rocks as they crystallize and cool are parallel or subparallel to solid-phase oxygen buffers such as QFM (quartz-fayalite-magnetite) or NNO (e.g., Haggerty, 1976; Sato, 1978; Sato & Valenza, 1980). The  $f_{\text{O}_2}$ s of initial Stillwater and Bushveld magmas are not well-established. Intrinsic  $f_{\text{O}_2}$  measurements suggest that the Bushveld Critical Zone and the Stillwater below the Howland Reef crystallized in environments in which  $f_{\text{O}_2}$ s were 3 to 7 orders of magnitude below NNO at equivalent temperatures (Elliot *et al.*, 1982; Buntin *et al.*, 1985). Although the veracity of these measurements is open to question (Ulmer *et al.*, 1987), recent determinations of  $\text{Fe}^{2+}/\text{Fe}^{3+}$  in submarine basalt glasses suggest that MORB magmas are 1.5 to 3 orders of magnitude more reduced than NNO (Christie *et al.*, 1986). Reduced conditions are also inferred from the amounts of carbon in vapor-glass inclusions in phenocrysts in these MORB glasses (Mathez & Delaney, 1981). Therefore, the possibility that Stillwater and Bushveld magmas were relatively reduced is not unreasonable from the point of view of what is known about oxidation states in rapidly quenched and undegassed lavas.

The presence of igneous graphite in the Critical Zone of the Bushveld requires that the  $f_{\text{O}_2}$  was somewhat more reduced than NNO. The precise  $f_{\text{O}_2}$  at which graphite becomes stable depends in part on pressure. Sharpe & Snyman (1980) estimated that the Critical Zone crystallized at a pressure of 4.1 kb. If graphite began crystallizing at 4 kb and 1050°C, the maximum  $f_{\text{O}_2}$  would have been  $10^{-12.2}$ , or 2.8 orders of magnitude below NNO (NNO - 2.8) and 2.0 orders of magnitude below QFM. Were  $\log f_{\text{O}_2} = \text{NNO} - 1.8$ , graphite would not have become stable until the temperature reached 750°C, which is probably below the solidus. The pressure of crystallization at the base of the Stillwater Complex is estimated to be 3-4 kb from the metamorphic assemblage in the pelitic floor rocks (Vaniman *et al.*, 1980; Labotka, 1985). If the Howland reef crystallized at 3 kb, at 1050°C the maximum  $f_{\text{O}_2}$  of graphite stability is  $10^{-12.3}$  (NNO - 2.9).

### *The evolution of vapor*

Based on the above considerations, it is suggested that the first vapors to have exsolved from Stillwater and Bushveld intercumulus magmas were essentially  $\text{CO}_2$ -CO mixtures in which were dissolved 4-6% sulfur species and unknown but probably large amounts of chlorine species. These initial vapors would have contained little or no water if their chlorine/hydrogen ratios were  $> 1$ , in which case most hydrogen would have been combined as HCl. Small amounts of  $\text{Cl}_2$  and  $\text{COCl}_2$  may also have been present (Fig. 6b).

Consider a model system in which the first vapor is assumed to exsolve at 1050°C, to be in equilibrium with graphite at a  $\log f_{\text{O}_2} = \text{NNO} - 2.8$ , and to contain 5 at.% hydrogen and 10 at.% chlorine. The evolution of the composition of such a vapor as it cools along an  $f_{\text{O}_2}$  isopleth of NNO - 2.8 is illustrated in Figs. 7 and 8. Several interesting features of this evolution are evident. First, as can be seen in Fig. 7, the  $\text{H}_2\text{O}$  content does not exceed that of either HCl or  $\text{CH}_3\text{Cl}$  until the system has cooled to below 975°C or that of  $\text{CO}_2$  until the temperature has reached 925°C. Second, with the exception of a continuous drop in  $\text{CO}_2$  contents, the vapor composition does not change dramatically with cooling below 950°C or so. Third,  $\text{CH}_4$  contents are strongly depressed through a wide subsolidus temperature range by stabilization of  $\text{CH}_3\text{Cl}$ .

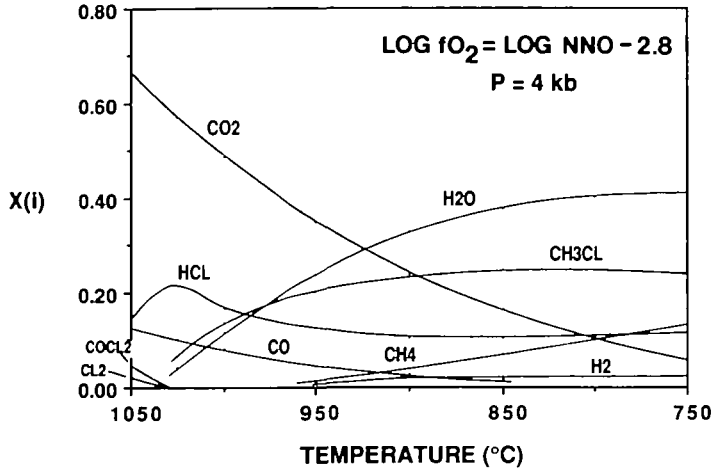


FIG. 7. The change in composition and speciation of graphite-saturated model fluid (see text) as it cools down an oxygen isopleth of  $\log f_{O_2} = \log NNO - 2.8$ . The chlorine content is constant at 10 at. %.

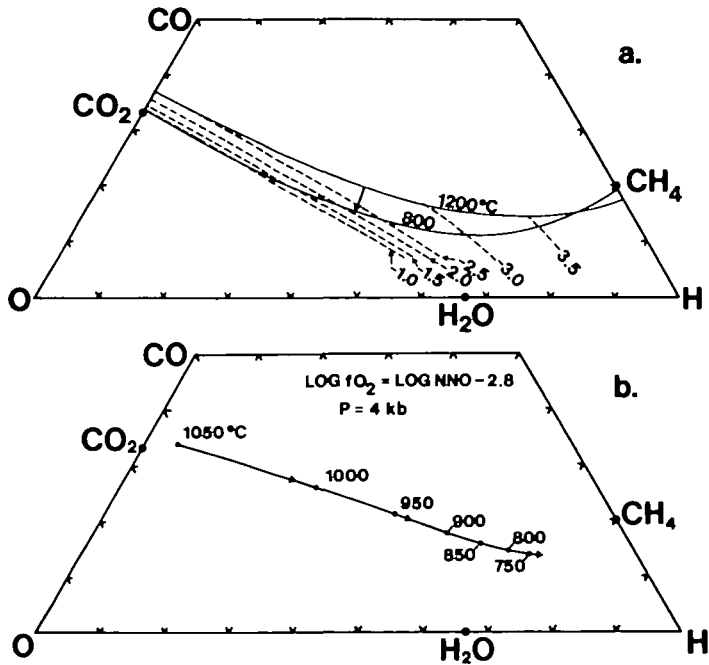


FIG. 8. (a) The relationship between the graphite stability curve and oxygen isopleths in the C-O-H system at 4 kb. Isopleths are labeled in log units relative to QFM. (b) The evolution of the model fluid projected onto the C-O-H face from the Cl apex. The evolution path represents the trace with cooling of the intersection of the graphite stability curve and the isopleth of  $\log f_{O_2} = \log NNO - 2.8$ , and the rapid change in composition results because these two curves intersect at a small angle.



The chemical evolution of the vapor is *driven entirely by graphite precipitation* because the graphite stability curve and the oxygen isopleths impinge on each other with cooling (Fig. 8a). The relative orientations of these curves results in two important features of vapor-graphite equilibria: *With cooling, the composition of the vapor is rapidly driven toward H<sub>2</sub>O* (Fig. 8b), and *graphite precipitation initially proceeds at an extremely rapid rate which progressively decreases with cooling* (Fig. 9). Thus, cooling of the model vapor from 1050 to 1025°C results in precipitation of 76% of the total mass of carbon initially in the vapor (Fig. 9). This is accompanied by a decrease in the mass of the vapor to about 28% of the original mass. Cooling an additional 25°C results in the precipitation of 10% more graphite and reduction of the mass to 18% of its original. These changing rates are mirrored by the initially rapid and then progressively decreasing rate of change in vapor composition with cooling illustrated on Fig. 8b.

An interesting consequence of this behavior is that in a narrow cooling interval the fugacities of the chlorine and sulfur species in the residual fluid are driven to higher values, which means that coexisting melts should become enriched in chlorine. Thus, this could explain the general association of chlorine-rich apatite and graphite in the Bushveld Critical Zone. Apatite crystallized from the melt as graphite precipitated and when fluid H<sub>2</sub>O fugacities were relatively low (Fig. 7). In fact, it is emphasized that due to the extremely low solubility of carbon in basaltic melt, the only realistic means of accounting for the massive graphite in the Critical Zone is by its precipitation from the fluid. Aside from graphite precipitation, the particular circumstance that permitted chlorine-rich apatite to form was that the mass of vapor was large in comparison to the mass of melt, i.e. that the melt and vapor evolved in an intercumulus environment and the vapors were concentrated at specific horizons in the Bushveld Upper Critical Zone and Stillwater Lower Banded Series. Phlogopite crystallized at lower temperature, after the H<sub>2</sub>O activity of the melt was driven to a much higher value in response to its increased fugacity in the fluid. (The reason why volatiles concentrated themselves in specific horizons in the crystallizing cumulate piles is not at this point clear. Again, that they did is simply indicated by the modal and textural characteristics of the rocks, as noted previously.)

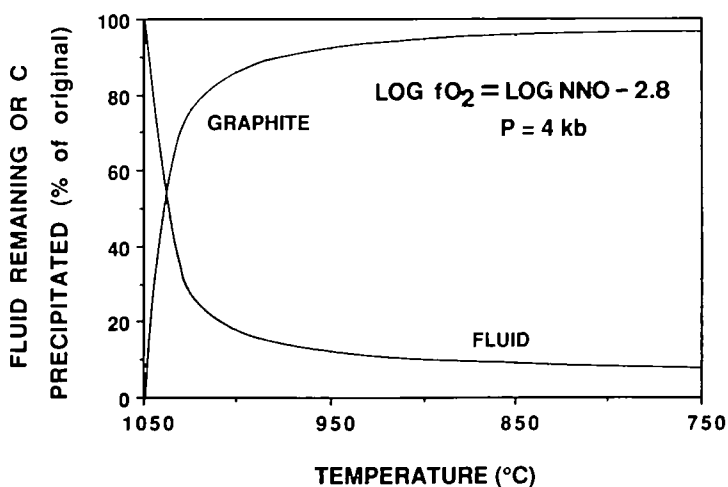


FIG. 9. The changes with cooling in mass proportions of carbon precipitated relative to the initial amount of carbon in the fluid ('graphite') and the fluid remaining relative to its initial mass ('fluid'). The calculation is for the model composition (see text).

Graphite precipitation should also result in the exsolution of sulfide melt. The amount of sulfide that could form this way will obviously be limited by the low concentration of sulfur in the vapor. However, the process is of interest because it means that not all sulfide in graphite-bearing horizons need have formed by the settling out of immiscible sulfide droplets from overlying magma.

Several points should be emphasized about this general model. First, a basic assumption is that the whole mineral–melt–vapor assemblage cools down a  $T$ - $f_{O_2}$  path parallel to one of the solid-phase buffers (Fig. 8a), i.e. that the condensed phases represent an infinite sink for the oxygen liberated by the fluid as it evolves along the path shown in Fig. 8b. Although the point was made above that cooling in this manner appears to be the general behavior of basaltic systems, there are processes that may cause them to behave differently. [For a more detailed discussion of this issue, see Mathez (1988).] For example, it has been asserted that redox conditions in some of the Critical Zone rocks were controlled during cooling by the vapor (Ballhaus & Stumpfl, 1985). There is no evidence for this in the rocks, however. In slowly cooled rocks, excursions from ambient  $f_{O_2}$  resulting from reactions involving fluid must be localized and ephemeral owing to the much larger mass of the silicate-oxide assemblage compared to that of the fluid on outcrop scales. Second, the model's veracity does not depend on Stillwater or Bushveld magmas being highly reduced but only that they were sufficiently reduced so that graphite appeared above the solidus. For example, if the Critical Zone solidus was 850°C, then the maximum  $f_{O_2}$  attendant on crystallization was NNO–2.1 (QFM–1.3), which, as noted above, is not unreasonably low. A carbon-rich, more oxidized vapor would encounter the graphite-saturation surface at a lower temperature but evolve in the same manner as the model one described above. Possibly the 'stockwork' Stillwater graphite and that in the Bushveld pipes precipitated in the subsolidus but in a manner analogous to that proposed for igneous graphite. Third, it is doubtful that vapor evolves only by graphite precipitation. In particular, the vapor H<sub>2</sub>O content should increase due to crystallization of anhydrous phases from the intercumulus melt. However, this effect should be overwhelmed by the effect of graphite during the initial stages of precipitation.

## CONCLUSION

The Stillwater OB I rocks typically contain 500–700 ppm carbon, depending on lithology, and are enriched in carbon compared to similar lithologies higher in the complex. Although the distribution of carbon was influenced locally by metamorphism, no evidence has been found to suggest large-scale redistribution. Therefore, the high carbon content of the Lower Banded Series troctolites is interpreted as an inherited feature of igneous processes.

The first vapor to exsolve from intercumulus melts in the lower portions of the Stillwater and Bushveld Complexes consisted of mixtures of CO<sub>2</sub>, CO, and HCl and contained little H<sub>2</sub>O. The evolution of such vapors probably reflected initial magma compositions in which chlorine/alkali ratios were relatively high. The evolution with cooling of the intercumulus melt–vapor system with respect to the volatile elements was controlled by graphite precipitation rather than by crystallization of silicate or oxide minerals. The precipitation of large masses of graphite relative to the initial masses of vapor over a narrow temperature interval resulted in strong enrichment of the vapor–melt system in the elements originally dissolved in the vapor and thus in crystallization of chlorine-rich apatite. The presence of igneous graphite in the Bushveld Critical Zone and possibly in the Stillwater Lower Banded Series implies that  $f_{O_2}$ s were < NNO–2.0.

The gross stratigraphy of layered intrusions reflects a chemical evolution by fractional

crystallization. Implicit in this understanding is that the volatile elements concentrate themselves at the tops of evolving magma chambers. However, it is in the lower portions of the Bushveld and Stillwater sections that evidence for volatile activity exists. The paradox is that carbon, one of the most volatile of elements in the magmatic environments, separates as graphite in reduced mafic systems at supersolidus temperature and thus is not always volatile. As the element that dominates and controls the formation of the first vapor to exsolve from magmas, it also controls the distribution of other elements, such as chlorine, that are partitioned into that vapor. But the precipitation of graphite from fluid is accompanied by enrichment of these volatile elements in the coexisting condensed phases rather than at the tops of intrusions.

#### ACKNOWLEDGEMENTS

We thank I. S. McCallum, B. R. Frost, G. Cawthorn, D. D. Lambert, C. G. Ballhaus, D. Pohl and B. W. Evans for their critical reviews. This paper was greatly improved as a consequence. This work was completed in part during a stay by EAM at the Laboratoire de Géochimie des Isotopes Stables, Université de Paris 7 and Institut de Physique du Globe, Paris. It was supported by NSF grant EAR-8409834. These institutions are gratefully acknowledged.

#### REFERENCES

- Allen, J. M., & Fawcett, J. J., 1982. Zoisite-anorthite-calcite stability relations in  $H_2O-CO_2$  fluids at 5000 bars: An experimental and SEM study. *J. Petrology* **23**, 215-39.
- Anderson, A. T., 1974. Chlorine, sulfur and water in magmas and oceans. *Bull. Geol. Soc. Am.* **85**, 1485-92.
- Ballhaus, C. G., 1988. Potholes of the Merensky Reef at Brakspruit shaft, Rustenburg Platinum Mines—primary disturbances in the magmatic stratigraphy. *Econ. Geol.* **83**, 1140-58.
- Stumpfl, E. F., 1985. Occurrence and petrological significance of graphite in the Upper Critical Zone, western Bushveld Complex, South Africa. *Earth planet. Sci. Lett.* **74**, 58-68.
- — 1986. Sulfide and platinum mineralization in the Merensky Reef: Evidence from hydrous silicates and fluid inclusions. *Contr. Miner. Petrol.* **94**, 193-204.
- Bergman, S. C., & Dubessy, J., 1984.  $CO_2-CO$  fluid inclusions in a composite peridotite xenolith: implications for upper mantle oxygen fugacity. *Ibid.* **85**, 1-13.
- Boudreau, A. E., Mathez, E. A., & McCallum, I. S., 1986. Halogen geochemistry of the Stillwater and Bushveld Complexes: Evidence for transport of the platinum-group elements by Cl-rich fluids. *J. Petrology* **27**, 967-86.
- McCallum, I. S., 1986. Investigations of the Stillwater Complex, Part III: The Picket Pin Pt/Pd deposit. *Econ. Geol.* **81**, 1953-75.
- Buntin, T. J., Grandstaff, D. E., Ulmer, G. C., & Gold, D. P., 1985. A pilot study of geochemical and redox relationships between potholes and adjacent normal Merensky Reef of the Bushveld Complex. *Econ. Geol.* **80**, 975-87.
- Burnham, W. C., 1979. The importance of volatile constituents. In: Yoder, H. S., Jr. (ed.) *The Evolution of Igneous Rocks, Fiftieth Anniversary Perspectives*. Princeton, N.J.: Princeton University Press, 439-82.
- Carmichael, I. S. E., & Ghiorso, M. S., 1986. Oxidation-reduction relations in basic magma: a case for homogeneous equilibria. *Earth planet. Sci. Lett.* **78**, 200-10.
- Christie, D. M., Carmichael, I. S. E., & Langmuir, C. H., 1986. Oxidation states of mid-ocean ridge basalt glasses. *Ibid.* **79**, 397-411.
- Devine, J. D., Sigurdsson, H., Davis, A. N., & Self, S., 1984. Estimates of sulfur and chlorine yield to the atmosphere from volcanic eruptions and potential climatic effects. *J. geophys. Res.* **89**, 6903-25.
- Dunn, T., 1986. An investigation of the oxygen isotope geochemistry of the Stillwater Complex. *J. Petrology* **27**, 987-97.
- Elliott, W. C., Grandstaff, D. E., Ulmer, G. C., Buntin, T., & Gold, D. P., 1982. An intrinsic oxygen fugacity study of platinum-carbon associations in layered intrusions. *Econ. Geol.* **77**, 1493-510.
- Falloon, T. J., & Green, D. H., 1986. Glass inclusions in magnesian olivine phenocrysts from Tonga: Evidence for highly refractory parental magmas in the Tonga arc. *Earth planet. Sci. Lett.* **81**, 95-103.
- Frost, B. R., 1985. On the stability of sulfides, oxides, and native metals in serpentinite. *J. Petrology* **26**, 31-63.
- Gerlach, T. M., & Nordlie, B. E., 1971. The C-O-H-S gaseous system, Part I: Composition limits and trends in basaltic gases. *Am. J. Sci.* **275**, 353-76.

- Gordon, S., & McBride, B. J., 1971. Computer program for calculation of complex equilibrium compositions, rocket performance, incident and reflected shocks, and Chapman-Jouquet detonations. NASA Sp. Publ., 273, 245 pp.
- Haggerty, S. E., 1976. Opaque mineral oxides in terrestrial igneous rocks. In: Rumble, D., III (ed.) *Oxide Minerals Short Course Notes*, v.3. Washington, D.C.: Mineral. Soc. Am., 101-301.
- Holloway, J. R., 1981. Volumes and compositions of supercritical fluids. In: Hollister, L. S., & Crawford, M. L. (eds) *Fluid inclusions: Petrologic applications*. Mineral. Assoc. Canada Short Course Handbook 6, 13-38.
- 1984. Graphite-CH<sub>4</sub>-H<sub>2</sub>O-CO<sub>2</sub> equilibria at low-grade metamorphic conditions. *Geology* 12, 455-8.
- Reese, R. L., 1974. The generation of N<sub>2</sub>-CO<sub>2</sub>-H<sub>2</sub>O fluids for use in hydrothermal experimentation I. Experimental method and equilibrium calculations in the C-O-H-N system. *Am. Miner.* 59, 587-97.
- Irving, A. J., & Mathez, E. A., 1982. The origin of glass in ultramafic xenoliths. *Terra Cognita* 2, 243.
- Iwasaki, B., & Katsura, T., 1967. The solubility of hydrogen chloride in volcanic rock melts at a total pressure of one atmosphere and at temperatures of 1200°C and 1290°C under anhydrous conditions. *Bull. Chem. Soc. Japan* 40, 554-61.
- Labotka, T. C., 1985. Petrogenesis of metamorphic rocks beneath the Stillwater Complex: Assemblages and conditions of metamorphism. In: Czamanske, G. K., & Zientek, M. L. (eds) *The Stillwater Complex, Montana: Geology and Guide*. Butte, Mt.: Montana Bureau of Mines and Geology Sp. Publ. 92, 70-6.
- Lauder, W. R., 1970. Origin of the Merensky Reef. *Nature* 227, 365-6.
- Mathez, E. A., 1976. Sulfur solubility and magmatic sulfides in submarine basalt glass. *J. geophys. Res.* 81, 4269-76.
- 1984. Influence of degassing on oxidation states of basaltic magmas. *Nature* 310, 371-5.
- 1987. Carbonaceous matter in mantle xenoliths: Composition and relevance to the isotopes. *Geochim. Cosmochim. Acta* 51, 2339-47.
- 1988. The nature of vapor associated with mafic magma and controls on its composition. In: Naldrett, A. J. & Whitney, J. (eds) *Ore Deposition Associated with Magmas*. Soc. Economic Geologists Short Course Notes (in press).
- Delaney, J. R., 1981. The nature and distribution of carbon in submarine basalts and peridotite nodules. *Earth planet. Sci. Lett.* 56, 217-32.
- Dietrich, V. J., & Irving, A. J., 1984. The geochemistry of carbon in mantle peridotites. *Geochim. Cosmochim. Acta* 48, 1849-59.
- McCallum, I. S., Raedeke, L. D., & Mathez, E. A., 1980. Investigations of the Stillwater Complex. Part I. Stratigraphy and structure of the Banded zone. *Am. J. Sci.* 280A, 59-87.
- Moore, J. G., Batchelder, J. N., & Cunningham, C. G., 1977. CO<sub>2</sub>-filled vesicles in mid-ocean basalt. *J. Volcanol. geotherm. Res.* 2, 309-27.
- Moore, J. G., & Fabbi, B. P., 1971. An estimate of the juvenile sulfur contents of basalts. *Contr. Miner. Petrol.* 33, 118-27.
- Pineau, F., Javoy, M., & Bottinga, Y., 1976. <sup>13</sup>C/<sup>12</sup>C ratios of rocks and inclusions in popping rocks of the mid-Atlantic Ridge and their bearing on the problem of isotopic composition of deep-seated carbon. *Earth planet. Sci. Lett.* 29, 413-21.
- Prausnitz, J. M., Lichtenthaler, R. M., & de Azvedo, E. G., 1986. *Molecular Thermodynamics of Fluid Phase Equilibria*. New York: Prentice-Hall.
- Raedeke, L. D., & McCallum, I. S., 1984. Investigations in the Stillwater Complex. Part II. Petrology and petrogenesis of the Ultramafic Series. *J. Petrology* 25, 390-420.
- Sato, M., 1978. Oxygen fugacity of basaltic magmas and the role of gas-forming elements. *Geophys. Res. Lett.* 5, 447-9.
- Valenza, M., 1980. Oxygen fugacities of the layered series of the Skaergaard Intrusion, East Greenland. *Am. J. Sci.* 280A, 134-58.
- Schiffries, C. M., 1982. The petrogenesis of a platinumiferous dunite pipe in the Bushveld Complex: Infiltration metasomatism by a chloride solution. *Econ. Geol.* 77, 1439-53.
- Schneiderhöhn, H., 1929. The mineralography, spectrography, and genesis of the platinum-bearing nickel-pyrrhotite ores of the Bushveld complex. In: Wagner, P. A. (ed.) *Platinum Deposits and Mines of South Africa*. London: Oliver and Boyd, 206-46.
- Sharpe, M. R., & Snyman, J. A., 1980. A model for the emplacement of the eastern compartment of the Bushveld Complex. *Tectonophysics* 65, 85-110.
- Sigvaldason, G. E., & Oskarsson, N., 1976. Chlorine in basalts from Iceland. *Geochim. Cosmochim. Acta* 40, 777-89.
- 1986. Fluorine in basalts from Iceland. *Contr. Miner. Petrol.* 94, 263-71.
- Sixta, V., 1977. Coulometric determination of carbonates in rock samples. *Z. Anal. Chem.* 285, 369-72.
- Stolper, E., & Holloway, J. R., 1988. Experimental determination of the solubility of carbon dioxide in molten basalt at low pressure. *Earth planet. Sci. Lett.* 87, 397-408.
- Stumpff, E. F., & Rucklidge, J. C., 1982. The platinumiferous dunite pipes of the eastern Bushveld Complex. *Econ. Geol.* 77, 1419-31.
- Trommsdorff, V., & Evans, B. W., 1977. Antigorite-ophicarbonates: Contact metamorphism in Valmalenco, Italy. *Contr. Miner. Petrol.* 62, 301-12.
- Ulmer, G. C., Grandstaff, D. E., Weiss, D., Moats, M. A., Buntin, T. J., Gold, D. P., Hatton, C. J., Kadik, A., Koseluk, R. A., & Rosenhauer, M., 1987. The mantle redox story: an unfinished story. In: Morris, E. M., & Pasteris, J. D. (eds) *Mantle Metasomatism and Alkaline Magmatism*. Geol. Soc. Amer. Spec. Paper 215, 5-23.

- Unni, C. K., & Schilling, J. G., 1978. Cl and Br degassing by volcanism along the Reykjanes Ridge and Iceland. *Nature* **272**, 19–23.
- Vaniman, D. T., Papike, J. J., & Labotka, T., 1980. Contact-metamorphic effects of the Stillwater Complex, Montana: the concordant iron formation. *Am. Miner.* **65**, 1087–102.
- Vermaak, C. F., 1976, The Merensky reef—thoughts on its environment and genesis. *Econ. Geol.* **71**, 1270–98.
- Viljoen, M. J., & Scoon, R. N., 1985. The distribution and main geologic features of discordant bodies of iron-rich ultramafic pegmatite in the Bushveld Complex. *Econ. Geol.* **80**, 1109–28.
- Volborth, A. A., & Housley, R. M., 1984. A preliminary description of complex graphite, sulphide, arsenide, and platinum group element mineralization in a pegmatoid pyroxenite of the Stillwater Complex, Montana, U.S.A. *Tschermaks Miner. Petrogr. Mitt.* **33**, 213–30.
- Wagner, P. A., 1924. On magmatic nickel deposits of the Bushveld igneous complex in the Rustenburg District of the Transvaal. *South African Geol. Survey Mem.* **21**, 181 p.
- Webster, J. D., & Holloway, J. R., 1988. Experimental constraints on the partitioning of Cl between topaz rhyolite melt and H<sub>2</sub>O and H<sub>2</sub>O+CO<sub>2</sub> fluids: New implications for granitic differentiation and ore deposition. *Geochim. Cosmochim. Acta* **52**, 2091–105.